

Physics

Physics Research Publications

Purdue University

Year 2010

Radio/gamma ray time delay in the
parsec-scale cores of active galactic nuclei

A. B. Pushkarev

Y. Y. Kovalev

M. L. Lister

This paper is posted at Purdue e-Pubs.

http://docs.lib.purdue.edu/physics_articles/1312

RADIO/GAMMA-RAY TIME DELAY IN THE PARSEC-SCALE CORES OF ACTIVE GALACTIC NUCLEI

A. B. PUSHKAREV^{1,2,3}, Y. Y. KOVALEV^{1,4}, AND M. L. LISTER⁵

¹ Max-Planck-Institut für Radioastronomie, Auf dem Hügel 69, 53121 Bonn, Germany; apushkar@mpifr.de

² Pulkovo Observatory, Pulkovskoe Chaussee 65/1, 196140 St. Petersburg, Russia

³ Crimean Astrophysical Observatory, 98409 Nauchny, Crimea, Ukraine

⁴ Astro Space Center of Lebedev Physical Institute, Profsoyuznaya 84/32, 117997 Moscow, Russia; yyk@asc.rssi.ru

⁵ Department of Physics, Purdue University, 525 Northwestern Avenue, West Lafayette, IN 47907, USA; mlister@purdue.edu

Received 2010 June 9; accepted 2010 August 19; published 2010 September 16

ABSTRACT

We report the detection of a non-zero time delay between radio emission measured by the VLBA at 15.4 GHz and γ -ray radiation (γ -ray leads radio) registered by the Large Area Telescope (LAT) on board the *Fermi Gamma-Ray Space Telescope* for a sample of 183 radio and γ -ray bright active galactic nuclei. For the correlation analysis, we used 0.1–100 GeV γ -ray photon fluxes, taken from monthly binned measurements from the first *Fermi* LAT catalog, and 15.4 GHz radio flux densities from the MOJAVE VLBA program. The correlation is most pronounced if the core flux density is used, strongly indicating that the γ -ray emission is generated within the compact region of the 15 GHz VLBA core. Determining the Pearson's r and Kendall's τ correlation coefficients for different time lags, we find that for the majority of sources the radio/ γ -ray delay ranges from 1 to 8 months in the observer's frame and peaks at approximately 1.2 months in the source's frame. We interpret the primary source of the time delay to be synchrotron opacity in the nuclear region.

Key words: galaxies: active – galaxies: jets – gamma rays: galaxies – radio continuum: galaxies

Online-only material: color figure, machine-readable table

1. INTRODUCTION

Long-term systematic observations of active galactic nuclei (AGNs) have produced detailed light curves that are a powerful tool for investigating the nature of these highly energetic phenomena. AGNs show variability across the full electromagnetic spectrum and multi-frequency monitoring programs serve to establish connections between flux variations at different energy bands.

The first comparison between long-term records of radio (10.7 GHz) and optical fluxes for a sample of 24 AGNs (Pomphrey et al. 1976) showed a correlation in only 13 sources, with the optical events preceding radio by intervals of 0–14 months. Subsequent analysis of light curves for 18 AGNs taken in the optical and radio (4.6–14.5 GHz) domains (Clements et al. 1995) demonstrated similar statistics: nine sources exhibited positive radio–optical correlations, with a time lag ranging from 0 to 14 months. Tornikoski et al. (1994) reported on a correlation in 10 out of 22 sources comparing optical and radio (22–230 GHz) observations. Remarkably, in six sources the variability was simultaneous. A more recent statistical study of the time delay between individual millimeter- and centimeter-wave flare peaks made by Hovatta et al. (2008) for a sample of 55 sources showed a large scatter of time lags that ranged up to several hundreds of days between 4.8 and 230 GHz, and tended to increase with decreasing radio frequency band. Jorstad et al. (2010) investigated the flaring behavior of the quasar 3C 454.3 and showed that optical outbursts led the 230 GHz flares by 15–50 days, confirming an earlier result by Raiteri et al. (2008), who found millimeter flux changes lagging behind the optical on a timescale of about 60 days. A longer delay of about 10 months between optical and 37 GHz radio flux variations was reported in this source by Volvach et al. (2008). Lähteenmäki & Valtaoja (2003) studied the connection between γ -ray emission detected by EGRET and phases of corresponding radio flares at 22 and 37 GHz. They reported that the highest levels of γ -ray emission were detected 30–70 days after the onset of the high-frequency radio flare.

The *Fermi Gamma-Ray Space Telescope*, successfully launched in 2008 June, has opened a new era in γ -ray astronomy. A number of AGN radio/ γ -ray connections have been established on the basis of the first three months of *Fermi* science operations and quasi-simultaneous very long baseline interferometry (VLBI) observations, namely, that the γ -ray photon flux correlates with the parsec-scale radio flux density (Kovalev et al. 2009), and that the jets of the Large Area Telescope (LAT) detected blazars have higher-than-average apparent speeds (median of 15 c ; Lister et al. 2009a), larger apparent opening angles (median of 20°; Pushkarev et al. 2009), and higher variability Doppler factors (mean of 20; Savolainen et al. 2010). In addition, AGN jets tend to be found in a more active radio state within several months of the LAT detection of their strong γ -ray emission (Kovalev et al. 2009). A significant correlation was detected even between non-simultaneous measurements of 0.1–100 GeV photon flux and 8 GHz Very Long Baseline Array (VLBA) flux density (Kovalev 2009). Nonetheless, there are several key questions that remain to be addressed, which include (1) the dominant production mechanism(s) of γ -ray photons, (2) the exact location of the high-energy emission, and (3) the nature of the AGN γ -ray duty cycle. In this Letter, we investigate the radio/ γ -ray time delays for parsec-scale jets and place constraints on the localization of the region where most of the γ -ray photons are produced.

Throughout this Letter, we use the term “core” as the apparent origin of AGN jets that commonly appears as the brightest feature in VLBI images of blazars (e.g., Lobanov 1998; Marscher 2008).

2. THE RADIO DATA AND SOURCE SAMPLE

The MOJAVE program (Lister et al. 2009b) is a long-term VLBA project to study the total intensity structure changes and polarization evolution of extragalactic relativistic radio jets in the northern sky. The observed sources include a statistically complete, flux-density-limited sample of 135 AGNs (MOJAVE-1). All the MOJAVE-1 sources have J2000 declina-

Table 1
Sample of LAT-detected MOJAVE AGNs

Source (1)	Alias (2)	<i>Fermi</i> Name (3)	z (4)	Redshift Reference (5)
0003 + 380	...	1FGL J0005.7 + 3815	0.229	Abdo et al. (2010c)
0015 – 054	...	1FGL J0017.4 – 0510	0.227	Abdo et al. (2010c)
0048 – 071	OB –082	1FGL J0051.1 – 0649	1.975	Abdo et al. (2010c)
0048 – 097	...	1FGL J0050.6 – 0928
0059 + 581	...	1FGL J0102.8 + 5827	0.644	Abdo et al. (2010c)
0106 + 013	4C +01.02	1FGL J0108.6 + 0135	2.099	Abdo et al. (2010c)
0106 + 678	4C +67.04	1FGL J0110.0 + 6806	0.290	Abdo et al. (2010c)
0109 + 224	...	1FGL J0112.0 + 2247	0.265	Abdo et al. (2010c)
0110 + 318	4C +31.03	1FGL J0112.9 + 3207	0.603	Abdo et al. (2010c)
0113 – 118	...	1FGL J0115.5 – 1132	0.672	Abdo et al. (2010c)

Notes. Columns are as follows: (1) IAU name (1950); (2) alternate name; (3) 1FGL name; (4) redshift; (5) literature reference for redshift.

(This table is available in its entirety in a machine-readable form in the online journal. A portion is shown here for guidance regarding its form and content.)

tion $\delta > -20^\circ$ and a 15 GHz VLBA correlated flux density $S_{\text{corr}} > 1.5$ Jy (2 Jy for $\delta < 0^\circ$) at any epoch between 1994.0 and 2004.0. The weaker radio blazars ($S_{\text{corr}} > 0.2$ Jy) detected by *Fermi* extend the complete MOJAVE-1 sample to MOJAVE-2. The monitoring list currently consists of 293 sources, 186 of which are members of the First *Fermi* LAT catalog (1FGL; Abdo et al. 2010a) that are positionally associated with AGNs. We note that the 186 sources do not represent a complete sample selected on either parsec-scale radio flux density or γ -ray photon flux.

3. RESULTS

3.1. Radio/ γ -ray Delay in VLBI Cores

Apart from the median γ -ray photon and energy fluxes, the 1FGL catalog provides flux history data, in the form of monthly binned 0.1–100 GeV photon flux measurements during the first 11 months of the *Fermi* scientific operations, which started on 2008 August 4. The time sampling of our VLBA radio observations is source dependent: objects with more rapid structural changes (i.e., faster apparent speeds) are observed more frequently. There are only five sources in our sample that are monitored with a cadence more frequent than once every two months. Starting in early 2009, fifty-five bright γ -ray detections ($>10\sigma$) from the *Fermi* LAT three-month list positionally associated with bright radio-loud blazars (Abdo et al. 2009a, 2009c; Kovalev 2009) have been incrementally added to the MOJAVE program. More than half of these new LAT-detected sources have fewer than three epochs of radio observations during the *Fermi* era, which precludes the correlation analysis of individual light curves. Therefore, our study is based upon a statistical approach.

Overall, we obtained 564 VLBA images and corresponding model fits for 183 bright γ -ray sources (Table 1) within a period from 2008 June to 2010 March. The parsec-scale structure, typically represented by a one-sided core-jet morphology, was fitted with the procedure *modelfit* in the Difmap package (Shepherd 1997) using a limited number of primarily circular Gaussian components, as described by Lister et al. (2009b).

We tested for possible correlations between the γ -ray photon fluxes and 15 GHz VLBA core flux densities using the following procedure: (1) we selected all pairs of measurements where the difference in the radio and γ -ray epochs lay within a restricted time interval, for instance, $[-0.5, +0.5]$ month, where the negative sign indicates that the radio measurement precedes the

γ -ray one; (2) if more than one pair of fluxes were available for a source, we selected the one with the epoch difference closest to the mean of the time interval. The procedure was then repeated iteratively by shifting the time interval by 0.5 months each time. We performed a quantitative analysis that confirmed that our data do not provide any bias toward positive pairs of radio/ γ -ray epoch difference. We used a cutoff of signal-to-noise ratio $S/N > 3$ for the γ -ray photon flux measurements to avoid a bias due to the lack of sources that are both weak in radio and γ -rays, and to exclude the influence of low-quality data points. For each data set, we calculated the Pearson's r and non-parametric Kendall's τ correlation coefficients, together with a corresponding probability of a chance correlation (Table 2). A non-zero radio/ γ -ray time lag, clearly seen as a bump in the correlation versus delay curves (Figure 1, left top panel), ranges from 1 to 8 months. The smooth fitted curves were obtained by applying a three-point moving average.

To test the robustness of this result, we estimated the uncertainty value of the correlation coefficients. Since both the radio flux densities and the γ -ray photon fluxes are far from being normally distributed, direct methods like the Fisher transformation or Student's t -distribution could not be used. Thus, we applied randomization techniques based on permutation tests to construct confidence intervals on the correlation coefficients. For each data set the randomization was done in the following manner: (1) we randomly swapped the radio measurements for one source with another source, keeping the γ -ray fluxes the same and (2) we calculated correlation coefficients r and τ from the randomized data. We then repeated these steps 2000 times. A 95% confidence interval (given in Table 2) for the correlation coefficients was defined as the interval spanning from the 2.5th to the 97.5th percentile of the re-sampled r and τ values. To estimate the null-basis level of the flux–flux correlation (which is present due to an overall radio/ γ -ray correlation; see Section 3.2), we shuffled the γ -ray photon fluxes among the 11 measurements available for every source, keeping the epoch dates and radio flux densities the same. The resulting values were $r_0 = 0.37$ and $\tau_0 = 0.26$ (Figure 1, left bottom panel). When we randomly selected 90% (and 80%) of the sample, the correlations remained significant, indicating that they are not driven by outliers. Additionally, we found no significant correlation between redshift and the VLBA core flux density averaged for the sample over the *Fermi* era.

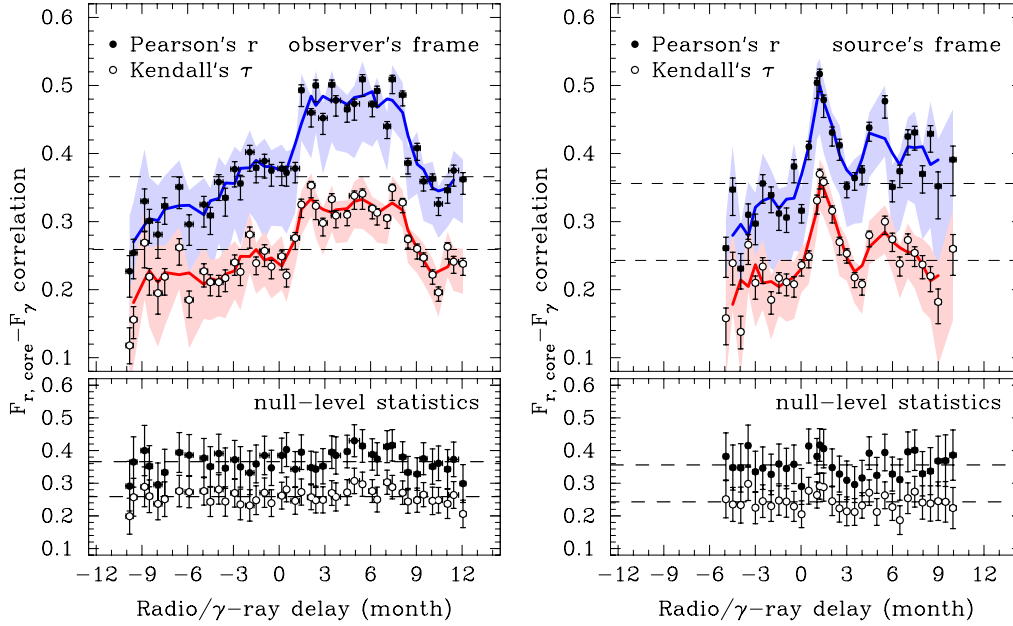


Figure 1. Left: upper panel: flux–flux correlation level as a function of the time interval between integrated 0.1–100 GeV photon flux and radio core flux density measurements in the observer’s frame. Filled circles represent the Pearson’s r statistic and open circles denote the Kendall’s τ statistic. The error bars are shown at the 68% level, while shaded areas represent 95% confidence regions. The thick curves are constructed by applying a three-point moving average. Dashed lines show the null-basis level of the correlation due to the overall γ -ray photon flux vs. radio flux density correlation. Lower panel: estimation of the null level correlation obtained by shuffling γ -ray photon fluxes for every source and keeping radio flux densities the same. Right: same curves, corrected to the source rest frame. A sharp peak at a delay of ~ 1.2 months is detected.

(A color version of this figure is available in the online journal.)

The wide range of delays in which the flux–flux correlations are significant (Figure 1, left) is presumably a result of the multiple parameters that determine the conditions in the nucleus (black hole mass, its spin, and accretion rate) and in the nearby interstellar medium. The delay is also affected by geometry, including the angle of the jets to our line of sight and the wide range of redshifts in our sample. The redshifts are known for more than 90% of the sources (166 out of 183). We re-did the analysis in the source’s frame by dividing the radio/ γ -ray epoch time difference for each source by a factor of $(1+z)$. This gave a typical time delay of ~ 1.2 months in the source frame (Figure 1, right), which corresponds to ~ 2.5 months (for $z \sim 1$) in the observer’s frame. The other sub-peaks are not significantly different from the null level of correlation, though they may indicate longer delays in a smaller number of sources. Note that the points on the radio/ γ -ray correlation curve are dependent. We expect the smearing even in the source frame delay because the core size is redshift dependent: more distant sources have higher rest-frame frequencies, and therefore should have a smaller core radius and shorter rest-frame delay. This effect can potentially be studied in more detail using a larger sample subdivided into high-redshift and low-redshift bins. Since a distribution of different delay values is expected, we do not estimate an error range on the detected peak. The peak value should only be taken as a typical one for the AGNs in our sample.

In Figure 2, we plot the integrated 0.1–100 GeV γ -ray photon flux against the 15 GHz VLBA core flux density for data pairs in which the γ -ray measurement leads the radio measurement by 2.5 ± 0.2 months in the observer’s frame. The formal probability of a chance correlation is 5×10^{-6} . If we drop the points with photon flux greater than 4×10^{-7} ph cm $^{-2}$ s $^{-1}$, the correlation is still present at a very high level of significance. We also note the span over one order of magnitude in the γ -ray fluxes for a given radio flux density. Several factors can contribute to this

scatter: the shape of the γ -ray spectrum, K -correction effects, different seed photons, and different Doppler boosting levels in the γ -ray and radio domains (Lister 2007).

3.2. Localization of the γ -ray Emission Region

Although radio-loud AGNs are generally known to have twin jet structures, the sources in our sample typically have a one-sided parsec-scale morphology (Lister et al. 2009b), implying strong selection effects and Doppler boosting of the jet emission. Localization of the γ -ray emission region within the AGN radio structure and its physical production mechanism(s) remain topics of active debate. There are three possibilities for the site of the high-energy emission: (1) only within the unresolved radio core, (2) only in the resolved (downstream) jet region, and (3) both in the core and jet.

Repeating the same analysis as in Section 3.1 for the total VLBA flux density, we found that the corresponding correlation coefficients agree within the 95% errors with those found for the core flux densities. Thus, no firm conclusions can be drawn out of this comparison. Indeed, the sources in our sample are highly core dominated, with a median value of $S_{\text{core}}/S_{\text{VLBA}} = 0.71$, where S_{core} and S_{VLBA} are the core and the total VLBA flux density, respectively. By contrast, when the jet flux densities ($S_{\text{VLBA}} - S_{\text{core}}$) are used, the correlation coefficients are significantly lower, making scenario (2) less probable. To reduce the uncertainty in the jet flux density estimations, we excluded sources with a high (>0.9) core dominance. Nevertheless, the correlation between the jet flux densities measured quasi-simultaneously with the γ -ray photon flux is still significant. This could be the result of both radio and γ -ray regimes being boosted by similar beaming factors (Lister et al. 2009a; Kovalev et al. 2009; Savolainen et al. 2010). Assuming the same Doppler factor for the jet and the core (opaque jet base), we would expect a weak but significant correlation between the jet flux density and integral γ -ray

Table 2
Radio/ γ -ray Flux–Flux Correlation Statistics for the VLBA Cores in the Source Frame

$\Delta t_{R-\gamma}$ (1)	N (2)	r (3)	τ (4)	p (5)
-4.9 ± 0.2	38	$0.26^{+0.04}_{-0.20}$	$0.16^{+0.06}_{-0.09}$	1.6×10^{-1}
-4.5 ± 0.2	50	$0.35^{+0.06}_{-0.11}$	$0.24^{+0.05}_{-0.07}$	1.4×10^{-2}
-4.0 ± 0.2	42	$0.23^{+0.07}_{-0.11}$	$0.14^{+0.06}_{-0.06}$	2.0×10^{-1}
-3.5 ± 0.1	54	$0.31^{+0.05}_{-0.11}$	$0.27^{+0.04}_{-0.07}$	4.5×10^{-3}
-3.0 ± 0.2	59	$0.30^{+0.04}_{-0.10}$	$0.21^{+0.04}_{-0.07}$	1.9×10^{-2}
-2.5 ± 0.1	58	$0.36^{+0.04}_{-0.11}$	$0.23^{+0.04}_{-0.06}$	9.4×10^{-3}
-2.0 ± 0.2	60	$0.34^{+0.04}_{-0.11}$	$0.18^{+0.04}_{-0.06}$	3.6×10^{-2}
-1.5 ± 0.1	70	$0.31^{+0.04}_{-0.09}$	$0.22^{+0.03}_{-0.06}$	8.0×10^{-3}
-1.0 ± 0.2	68	$0.31^{+0.05}_{-0.08}$	$0.21^{+0.03}_{-0.06}$	1.1×10^{-2}
-0.5 ± 0.1	76	$0.38^{+0.03}_{-0.12}$	$0.21^{+0.03}_{-0.05}$	7.9×10^{-3}
0.0 ± 0.2	90	$0.32^{+0.03}_{-0.06}$	$0.24^{+0.03}_{-0.04}$	9.6×10^{-4}
0.5 ± 0.1	95	$0.41^{+0.03}_{-0.10}$	$0.25^{+0.03}_{-0.04}$	3.5×10^{-4}
1.0 ± 0.1	85	$0.50^{+0.03}_{-0.08}$	$0.33^{+0.02}_{-0.05}$	7.3×10^{-6}
1.2 ± 0.1	87	$0.52^{+0.02}_{-0.09}$	$0.37^{+0.02}_{-0.05}$	4.0×10^{-6}
1.5 ± 0.1	83	$0.48^{+0.03}_{-0.08}$	$0.36^{+0.02}_{-0.05}$	1.6×10^{-6}
2.0 ± 0.1	91	$0.43^{+0.03}_{-0.07}$	$0.32^{+0.02}_{-0.04}$	9.0×10^{-6}
2.5 ± 0.1	89	$0.41^{+0.03}_{-0.07}$	$0.27^{+0.03}_{-0.05}$	1.8×10^{-4}
3.0 ± 0.1	96	$0.35^{+0.03}_{-0.06}$	$0.25^{+0.02}_{-0.04}$	2.6×10^{-4}
3.5 ± 0.1	100	$0.36^{+0.03}_{-0.07}$	$0.22^{+0.02}_{-0.04}$	1.3×10^{-3}
4.0 ± 0.2	98	$0.38^{+0.03}_{-0.08}$	$0.21^{+0.02}_{-0.04}$	2.4×10^{-3}
4.5 ± 0.1	99	$0.44^{+0.02}_{-0.07}$	$0.28^{+0.02}_{-0.04}$	4.1×10^{-5}
5.5 ± 0.1	86	$0.48^{+0.02}_{-0.08}$	$0.30^{+0.02}_{-0.05}$	4.4×10^{-5}
6.0 ± 0.2	82	$0.35^{+0.03}_{-0.07}$	$0.27^{+0.03}_{-0.05}$	2.6×10^{-4}
6.5 ± 0.2	77	$0.37^{+0.03}_{-0.09}$	$0.24^{+0.03}_{-0.05}$	2.2×10^{-3}
7.0 ± 0.2	74	$0.42^{+0.03}_{-0.09}$	$0.27^{+0.02}_{-0.06}$	5.8×10^{-4}
7.5 ± 0.2	72	$0.43^{+0.03}_{-0.10}$	$0.25^{+0.03}_{-0.05}$	1.6×10^{-3}
8.0 ± 0.2	63	$0.37^{+0.04}_{-0.10}$	$0.24^{+0.04}_{-0.07}$	6.0×10^{-3}
8.5 ± 0.2	58	$0.43^{+0.05}_{-0.14}$	$0.22^{+0.04}_{-0.06}$	1.5×10^{-2}
9.0 ± 0.2	42	$0.35^{+0.07}_{-0.16}$	$0.18^{+0.06}_{-0.09}$	8.9×10^{-2}
10.0 ± 0.2	38	$0.39^{+0.07}_{-0.20}$	$0.26^{+0.06}_{-0.10}$	2.1×10^{-2}

Notes. Columns are as follows: (1) radio–gamma time delay bin in months; (2) number of AGNs included in the bin; (3) Pearson’s r with uncertainties at a 95% confidence level; (4) Kendall’s τ with uncertainties at a 95% confidence level; (5) probability of a chance correlation.

emission. Alternatively, it is possible that for some low-redshift sources, γ -ray emission may also be produced outside the radio core, as could be the case in 3C 84 (Abdo et al. 2009b), where radio flare accompanying the γ -ray activity was detected in the innermost jet region.

We note that Kovalev (2009) found a correlation between the *Fermi* LAT 0.1–100 GeV photon flux from the three-month integration and 8 GHz radio flux density non-simultaneously measured by the VLBA. The presence of this correlation in this highly variable population further suggests that Doppler beaming is the likely cause, and that the Doppler factors of the individual jets are not changing substantially over time.

4. DISCUSSION

What is the main source of the detected time lag? Dispersion in the intervening medium cannot be responsible for a delay of several months. Our calculations following the Crab pulsar measurement by Abdo et al. (2010b) show that for an object at a redshift $z = 1$ the delay should not exceed a few seconds at 15 GHz.

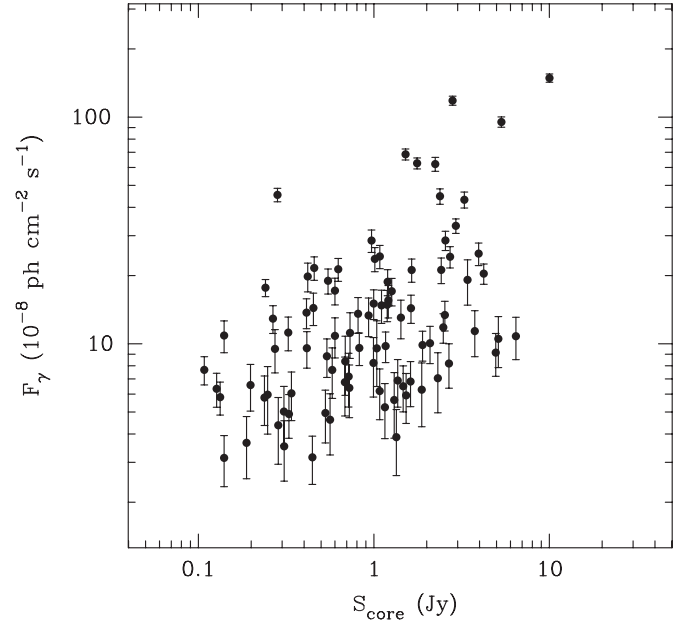


Figure 2. Integrated 0.1–100 GeV *Fermi* LAT photon flux vs. 15 GHz VLBA core flux density for data pairs in which the VLBA flux density measurement was taken 2.5 ± 0.2 months after the LAT flux measurements. One point is plotted per AGN.

The most likely source of the observed time lag is synchrotron opacity in the nuclear region. The radio core is optically thick to synchrotron emission up to the frequency-dependent radius $r_c \propto \nu^{-1}$ (Blandford & Königl 1979). This means that the γ -ray production region/zone is located upstream with respect to the 15 GHz apparent core position. Being induced by the same disturbance at a distance r_γ from the black hole, the radio and γ -ray emission at their peaks are not observed simultaneously due to the opacity effect. Although the γ -ray photons escape immediately, it takes several more months for the perturbation to propagate farther along the jet until it reaches the $\tau \simeq 1$ surface at 15 GHz radio emission (the radio core) and becomes detectable at radio frequencies. The corresponding distance traveled along the jet between the place where a γ -ray photon was emitted (r_γ) and the radius of the radio core (r_c) is

$$\Delta r = r_c - r_\gamma = \frac{\delta \Gamma \beta c \Delta t_{R-\gamma}^{\text{obs}}}{(1+z)}, \quad (1)$$

where δ is the Doppler factor, Γ is the Lorentz factor, βc is the intrinsic jet speed, and $\Delta t_{R-\gamma}^{\text{obs}}$ is the observed time delay. Using the relations for Doppler factor δ and apparent angular speed β_{app} (Cohen et al. 2007), the expression (1) can also be written in the form

$$\Delta r = \frac{\beta_{\text{app}} c \Delta t_{R-\gamma}^{\text{sour}}}{\sin \theta}, \quad (2)$$

where β_{app} is the apparent jet speed, $\Delta t_{R-\gamma}^{\text{sour}}$ is the radio to γ -ray time delay in the source’s frame, and θ is the viewing angle. Since we cannot measure radio/ γ -ray time delays for the sources individually from our data, let us consider a source with a set of parameters typical for a LAT-detected radio-loud blazar: apparent jet speed $\beta_{\text{app}} \sim 15$ (Lister et al. 2009a), viewing angle $\theta \sim 3^\circ 6$ (Pushkarev et al. 2009; Hovatta et al. 2009), and a typical time lag of 1.2 months in the source’s frame. Under these assumptions, we obtain the distance between the γ -ray production zone and the $\tau \approx 1$ surface at 15 GHz, the radio

core, $\Delta r \sim 7$ pc, which corresponds to a projected distance of ~ 0.9 pc, or ~ 0.1 mas for a source at $z \sim 1$. These estimates are consistent with the core radius obtained from the frequency-dependent core shift measurements (Lobanov 1998; Kovalev et al. 2008a, 2008b; O’Sullivan & Gabuzda 2009). This indicates that VLBI observations at higher frequencies, for instance at 43 GHz and 86 GHz, should register shorter delay or even quasi-simultaneous flux variations with γ -ray flux at least for some sources and might even resolve the region of the jet where γ -ray emission is generated.

The fact that the radio emitting region may be more physically extended than the γ -ray emission zone may also contribute to the detected delay. Finally, we note that our analysis is sensitive to the delay between the peaks at radio and γ -ray frequencies, but cannot address which flare, low-energy or high-energy, originates first. The latter analysis requires very well sampled light curves for a large set of γ -ray-detected AGNs.

5. SUMMARY

We have investigated the dependence between the integrated 0.1–100 GeV γ -ray photon flux and 15 GHz radio flux densities for a large sample of 183 LAT-detected AGNs observed by the VLBA within the MOJAVE program and concluded the following.

1. The correlation between γ -ray photon flux and radio flux density is found to be highly significant. The correlation analysis results for the core and the total VLBA flux density are indistinguishable. The correlation is systematically weaker if the jet flux density is used, providing further support for the localization of the γ -ray emission to the core region as well as a connection between the inverse-Compton γ -rays and the synchrotron radio emission from the jet.
2. We found a non-zero radio/ γ -ray delay (γ -ray leads the radio emission) that ranges from 1 to 8 months in the observer’s frame and peaks at ~ 1.2 months in the source frame. The delay is most likely connected with synchrotron opacity in the core region, although other mechanisms may play a role.
3. The region where most of γ -ray photons are produced is found to be located within the compact opaque parsec-scale core. The typical distance between the γ -ray production region and the 15 GHz radio core is estimated to be ~ 7 pc, which is consistent with the typical core radius derived from frequency-dependent core shift measurements.

These results are consistent with earlier findings reported by Kovalev et al. (2009) and Tavecchio et al. (2010) which place further constraints on the localization of the γ -ray production zone in parsec-scale jets. The MOJAVE program is continuing to monitor a large sample of LAT-detected AGNs for use in more comprehensive studies associated with the next *Fermi* data release.

We thank M. H. Cohen, K. I. Kellermann, E. Ros, T. Savolainen, and the rest of the MOJAVE team for useful

discussions. We thank the anonymous referee as well as A. Wehrle, T. Readhead, F. Tavecchio, and E. Valtaoja for useful comments. This research has made use of data from the MOJAVE database that is maintained by the MOJAVE team (Lister et al. 2009b). The MOJAVE project is supported under NSF grant AST-0807860 and NASA *Fermi* grant NNX08AV67G. Y.Y.K. was supported in part by the return fellowship of Alexander von Humboldt foundation and the Russian Foundation for Basic Research grant 08-02-00545. NRAO(VLBA) The VLBA is a facility of the National Science Foundation operated by the National Radio Astronomy Observatory under cooperative agreement with Associated Universities, Inc.

Facilities: VLBA, *Fermi* (LAT)

REFERENCES

- Abdo, A. A., et al. 2009a, *ApJ*, **700**, 597
 Abdo, A. A., et al. 2009b, *ApJ*, **699**, 31
 Abdo, A. A., et al. 2009c, *ApJS*, **183**, 46
 Abdo, A. A., et al. 2010a, *ApJS*, **188**, 405
 Abdo, A. A., et al. 2010b, *ApJ*, **708**, 1254
 Abdo, A. A., et al. 2010c, *ApJ*, **715**, 429
 Blandford, R. D., & Königl, A. 1979, *ApJ*, **232**, 34
 Clements, S. D., Smith, A. G., Aller, H. D., & Aller, M. F. 1995, *AJ*, **110**, 529
 Cohen, M. H., Lister, M. L., Homan, D. C., Kadler, M., Kellermann, K. I., Kovalev, Y. Y., & Vermeulen, R. C. 2007, *ApJ*, **658**, 232
 Hovatta, T., Niépola, E., Tornikoski, M., Valtaoja, E., Aller, M. F., & Aller, H. D. 2008, *A&A*, **485**, 51
 Hovatta, T., Valtaoja, E., Tornikoski, M., & Lähteenmäki, A. 2009, *A&A*, **498**, 723
 Jorstad, S. G., et al. 2010, *ApJ*, **715**, 362
 Kovalev, Y. Y. 2009, *ApJ*, **707**, L56
 Kovalev, Y. Y., Lobanov, A. P., & Pushkarev, A. B. 2008a, *Mem. Soc. Astron. Ital.*, **79**, 1153
 Kovalev, Y., Pushkarev, A., Lobanov, A., & Sokolovsky, K. 2008b, in *The Role of VLBI in the Golden Age for Radio Astronomy*, ed. F. Mantovani (Trieste: PoS), **7** (<http://pos.sissa.it/cgi-bin/reader/conf.cgi?confid=72>)
 Kovalev, Y. Y., et al. 2009, *ApJ*, **696**, L17
 Lähteenmäki, A., & Valtaoja, E. 2003, *ApJ*, **590**, 95
 Lister, M. L. 2007, in *AIP Conf. Ser. 921, The First GLAST Symposium*, ed. S. Ritz, P. Michelson, & C. A. Meegan (Melville, NY: AIP), **345**
 Lister, M. L., Homan, D. C., Kadler, M., Kellermann, K. I., Kovalev, Y. Y., Ros, E., Savolainen, T., & Zensus, J. A. 2009a, *ApJ*, **696**, L22
 Lister, M. L., et al. 2009b, *AJ*, **137**, 3718
 Lobanov, A. P. 1998, *A&A*, **330**, 79
 Marscher, A. P. 2008, in *ASP Conf. Ser. 386, Extragalactic Jets: Theory and Observation from Radio to Gamma Ray*, ed. T. A. Rector & D. S. De Young (San Francisco, CA: ASP), **437**
 O’Sullivan, S. P., & Gabuzda, D. C. 2009, *MNRAS*, **400**, 26
 Pomphrey, R. B., Smith, A. G., Leacock, R. J., Olsson, C. N., Scott, R. L., Pollock, J. T., Edwards, P., & Dent, W. A. 1976, *AJ*, **81**, 489
 Pushkarev, A. B., Kovalev, Y. Y., Lister, M. L., & Savolainen, T. 2009, *A&A*, **507**, L33
 Raiteri, C. M., et al. 2008, *A&A*, **491**, 755
 Savolainen, T., Homan, D. C., Hovatta, T., Kadler, M., Kovalev, Y. Y., Lister, M. L., Ros, E., & Zensus, J. A. 2010, *A&A*, **512**, A24
 Shepherd, M. C. 1997, in *ASP Conf. Ser. 125, Astronomical Data Analysis Software and Systems VI*, ed. G. Hunt & H. E. Payne (San Francisco, CA: ASP), **77**
 Tavecchio, F., Ghisellini, G., Bonnoli, G., & Ghirlanda, G. 2010, *MNRAS*, **405**, L94
 Tornikoski, M., Valtaoja, E., Terasranta, H., Smith, A. G., Nair, A. D., Clements, S. D., & Leacock, R. J. 1994, *A&A*, **289**, 673
 Volvach, A. E., Volvach, L. N., Larionov, M. G., Aller, M. F., Aller, H. D., Villata, M., & Raiteri, K. M. 2008, *Astron. Rep.*, **52**, 867